

# Temporal Pulse Shape Modulation in Single-Pass Solid State Amplifier

Ramon Springer, Christoph Pflaum

University of Erlangen-Nuremberg

Department of Computer Science 10 (LSS)

Erlangen Graduate School in Advanced Optical Technologies (SAOT)

Germany, Erlangen 91058

Email: ramon.springer@fau.de

**Abstract**—This paper demonstrates a one dimensional numerical model for single-pass solid state laser amplifiers. It is shown that after amplification the temporal shape of individual pulses within a pulse train can significantly vary, which results in an unstable interpulse spacing and a non reliable temporal pulse stability. Moreover possible adjustments of the pump pulse duration are pointed out in order to secure a stable temporal intensity output of the seed pulse train. In detail, the model is based on a non-linear time-dependent photon transport equations combined with a four level rate equations system and a pulsed end-pumping configuration.

## 1. Introduction

Solid state lasers that produce short pulses in the picosecond regime at gigahertz repetition rates are key components for photonic switching devices, high capacity telecommunication systems and high precision machining [1-3]. Especially the controlled ablation of material and the subsequent nanoparticle formation is strongly dependent on the intensity profile of laser pulses [4]. However, in order to realize short pulse laser systems the development of single-pass amplifier play an essential role to amplify the optical signal [5]. Key goals of a single-pass amplifier as part of a chirped-pulse-amplification system are to increase the energy of each pulse while maintaining a stable interpulse spacing and a constant temporal shape of each pulse that exits the amplifier [6]. Only then a reliable and efficient laser operation can be secured.

The population inversion for each pulse is determined by the previous seed pulse that entered the medium and the excitation of dopants by the pump pulse [7]. Consequently, the gain and temporal intensity shape for each individual seed pulse might show significant deviations compared to other seed pulses of the same pulse train [8]. Here, a numeric model of a single-pass amplifier is presented that propagates seed and pump pulses through the amplifying medium and calculates the gain and population inversion at time and space coordinates. Moreover, the model allows to determine the pump pulse and seed pulse parameters (energy, duration, repetition rate), which enable stable operation in terms of pulse stability and interpulse spacing.

## 2. Model

In order to simulate the propagation of laser pulses through the amplifying medium an Nd:YAG crystal is discretized in one dimension along the optical axis. Additionally the 1-D discretization is extended with a temporal axis which allows to track the time dependence of the population inversion and also the seed and pump pulse propagation. In order to adjust the resolution of the temporal and spatial axis the meshsize is calculated from the input seed pulse duration. Therefore, setting a seed pulse duration will automatically adjust the meshsize and enables high resolution sampling of input seed pulses with arbitrary temporal profiles.

In order to model the amplification of propagating pulses within the amplifier the non-linear time-dependent photon transport equation is used based on the theory by Frantz-Nodvik [9].

$$\frac{\partial n}{\partial t} + c \frac{\partial n}{\partial x} = \sigma_e c n \Delta_p \quad (1)$$

Here,  $n$  is the photon density,  $\sigma_e$  is the emission cross section,  $\Delta_p$  is the population inversion density,  $c$  is the light speed in the crystal while  $x$  and  $t$  are the space and time coordinates.

The transport equation is solved numerically by starting from the sampled seed pulse intensity as initial value. By rearranging (1) the following approach can be obtained, which represents a finite difference euler method .

$$n_{n+1}^{k+1} = n_i^k (1 + \sigma_e h \Delta_{p,i}^k) \quad (2)$$

Here, the amplified photon density at timestep  $k+1$  and grid coordinate  $x+1$  is calculated from the photon density and population inversion density at the previous timestep  $k$  and grid coordinate  $x$ . The meshsize is denoted with  $h$  and represents the spatial distance between two gridpoints.

In order to calculate the population inversion rate equations are employed to model charge transfer within a four level system [10,11]. Additionally, the absorption of pump pulses along the seed pulse direction is integrated into the present model [12].

### 3. Results

The following table displays the simulations parameters which resulted in the amplified seed pulse trains shown in Fig. 1 and Fig 2. The pulse durations for each seed and pump pulse are specified as  $t_{seed}$  and  $t_{pump}$  while the corresponding pulse energies are named  $E_{seed}$  and  $E_{pump}$ , respectively.

TABLE 1: Simulation Parameters

Fig. 1	$t_{seed}$	0.1 ns	$E_{seed}$	1 $\mu J$
	$t_{pump}$	0.1 ns	$E_{pump}$	100 $\mu J$
Fig. 2	$t_{seed}$	0.1 ns	$E_{seed}$	1 $\mu J$
	$t_{pump}$	1 ns	$E_{pump}$	100 $\mu J$

Both pulse trains (pump and seed) exhibit a repetition rate of 200 MHz and synchronously enter the crystal from the same direction. The seed and pump pulses have a Lorentzian temporal shape and propagate through a Nd:YAG crystal that has a length of 1 cm.

The exiting seed pulse trains in Fig. 1 and Fig. 2 are both characterized by their gain, interpulse spacing and their match to the temporal shape of the input seed pulses. In case of Fig. 1 a peak gain of 250 can be stated. Additionally, it can be seen that the output seed pulses have lost their initial Lorentzian shape and obtained a stretched temporal intensity profile. Consequently, a stable interpulse spacing is not existing since a temporal separation between single pulses does not occur over the entire output seed pulse train.

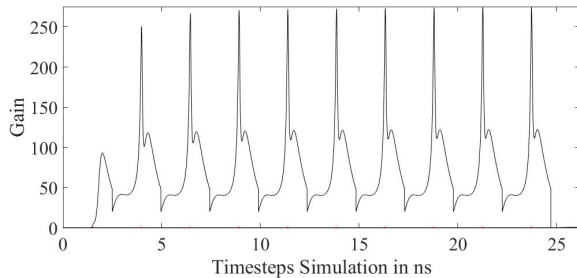


Fig. 1: Amplified seed pulse train pumped by pulses with 0.1 ns duration. The seed pulses show an unstable interpulse spacing and a strongly modulated temporal shape.

In contrast all amplified seed pulses which are displayed in Fig. 2 exhibit a Lorentzian temporal profile while maintaining a clear separation of single pulse. This results in a constant interpulse spacing over the entire seed pulse train and is due to the extended pump pulse duration from 0.1 ns to 1 ns. Since the energy of the pump pulses is kept constant but their temporal profile is stretched the propagating pump pulses exhibit less intensity. The absorption of pump light decreases exponentially with decreasing pump pulse intensity, which results in a lower population inversion inside the crystal compared to Fig. 1. Therefore, the peak gain of each seed pulse in Fig. 2 reaches a value of only 90 after six

pulses have passed the crystal. The first six seed pulses are less amplified since the population inversion rises by every injected pump pulse until a balance between excitation and radiative decay of the Nd dopant is reached.

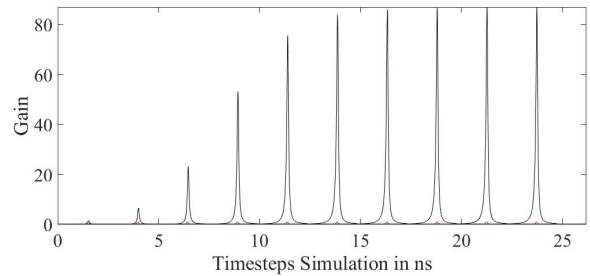


Fig. 2: Amplified seed pulse train pumped by pulses with 1 ns duration. The pulse train exhibits a stable interpulse spacing and preserved Lorentzian temporal shape.

Compared to Fig. 2 the pump pulses in Fig. 1 exhibit a ten times higher intensity. For that reason, the maximum gain is already attained after two pump pulses propagated through the crystal.

### 4. Conclusion

The model demonstrates that by increasing the pump pulse duration a Lorentzian temporal shape of the amplified seed pulses within a pulse train can be preserved. Consequently, a stable interpulse spacing can be achieved. Besides Nd:YAG the model is capable of simulating pulse trains through other solid-state amplifiers with various geometries. Further simulations are of interest that estimate temporal stable pulse amplification regimes depending on other four level or three level solid-state laser systems e.g. Ti:Sapphire or Yb:YAG, respectively.

### Acknowledgments

The authors gratefully acknowledge funding of the DFG (PF 372/10-1) and the SAOT.

### References

- [1] U. Keller, *Nature*, 424, 831-838, 2003
- [2] A. Esteban-Martin, M. Ebrahim-Zadeh, C. Pflaum, *Opt. Letters*, Vol. 34, No. 4, 2009.
- [3] L. Krainer, U. Keller, *IEEE J. of Quantum Electron.*, Vol. 38, No. 10, 2002.
- [4] A. Menendez-Manjón, B.N. Chichkov, *Laser and Particle Beams*, 28, 4552, 2010.
- [5] M. Hentschel, Ch. Spielmann, *Appl. Phys.* 70, 161164, 2000
- [6] B. Kohler, K. Wilson, *Optics Letters*, 20, 5, 1995
- [7] W. Warren, *J. Chem. Phys.* 81, 5437, 1984,
- [8] R. Stoian, I. V. Hertel, *Appl. Phys. A* 77, 265269, 2003
- [9] L. Frantz, J. Nodvik, *J. Appl. Physics*, 34, 2346, 1963.
- [10] O. Svelto, *Principles of Lasers*, Plenum Press, 4th ed., 1998.
- [11] I. Alexeev, C. Pflaum, *Eur. J. Phys.*, 37, 2016.
- [12] W. Koechner, *Solid State Laser Engineering*, Optical Sciences, 6th ed., 2010.